

Landslides (2023) 20:331–349
 DOI 10.1007/s10346-022-01963-y
 Received: 18 December 2021
 Accepted: 26 August 2022
 Published online: 15 September 2022
 © Springer-Verlag GmbH Germany,
 part of Springer Nature 2022

Wen-Jie Shiu · Ching-Fang Lee · Chia-Chi Chiu[✉] · Meng-Chia Weng ·
 Che-Ming Yang · Wei-An Chao · Chun-Yuan Liu · Cheng-Han Lin ·
 Wei-Kai Huang · GeoPORT Working Group



Analyzing landslide-induced debris flow and flow-bridge interaction by using a hybrid model of depth-averaged model and discrete element method

Abstract The Minbaklu Bridge, an essential segment of the southern cross-island expressway in Taiwan, was destroyed owing to debris flow in the Yusui Stream. To elucidate the development of debris flow in the Yusui Stream and the bridge collapse event, this study proposed a hybrid model of the discrete element method and depth-averaged model to simulate the event through three stages: formation of the natural dam, debris flow triggered by dam braking, and bridge collapse owing to the debris flow. The simulation results obtained indicate that the proposed model can provide reasonable simulations of the formation of natural dam in both time line and spatial distribution. Further, it indicated that the erosion developed at the river bed of the flow region, and illustrated the failure process of the Minbaklu Bridge, which revealed that it was uplifted before being pushed away. Furthermore, the final deposition of the alluvial fan deposition was demonstrated as well. Overall, the proposed hybrid model provides a useful tool for investigating debris flow and interaction with engineering structures.

Keywords Debris flow · Flow-structure interaction · Hybrid model · Depth-averaged model · Discrete element method

Introduction

The Minbaklu Bridge, an essential segment of the southern cross-island expressway in Taiwan, was destroyed owing to debris flow in Yusui Stream on August 7, 2021 (Fig. 1a, b) (Movie 1), which is triggered by the Typhoon Lupit. The failure of the newly established bridge garnered the attention of the public and resulted in more than 400 residents in the upstream area being isolated for 19 days. The 695-m-long bridge is located on a triple junction of the Laonong River and its two tributaries, Putanpunas Stream and Yusui Stream (Figs. 1c and 2). This bridge is a newly constructed part of the southern cross-island expressway because the original route was damaged by the debris flow of Putanpunas Stream during the Typhoon Morakot in 2009 (Lin and Lin 2015; Lo 2017; Lo et al. 2018). Consequently, the new bridge was built along the left bank of the Laonong River to avoid the impact of the debris flow of Putanpunas Stream. It is an appropriate selection because the threat of the Putanpunas Stream is more severe than that of the Yusui Stream (Fig. 2). However, the landslide upstream of the Yusui Stream (Silabaku Mountain) showed a potential threat to the downstream infrastructure.

In Taiwan, debris flow is a common disaster because of the heavy precipitation and fragile geological conditions. Lots of events occurred during the past decades such as Fonchu debris flow during Typhoon Herb and Songhe debris flow during Typhoon Mindulle (Lin and Jeng 2000; Chen and Petley 2005; Lin et al. 2011). In General, debris flow can be classified as gravel (sand and silt < 10%), normal, or mudflow (sand and silt > 50%) types. The gravel type is characterized by high impact forces, as exemplified by the Houyenshan gravelly gullies and Chen-Yu-Lan River in central Taiwan (Chen et al. 2006; Chang et al. 2011; Chou et al. 2013). The normal type of debris flow is commonly observed in other areas of Taiwan, such as the Putanpunas Stream in southern Taiwan (Jan and Chen 2005; Hsieh and Capart 2013; Chen 2016; Lee et al. 2016; Chou et al. 2017). However, expressway-level bridge failure accompanied by debris flow disasters is rarely found. Therefore, it is worthy to investigate this disaster and its consequences to the bridge failure.

Concerning the aspect of granular flow, some velocity distribution models considering the continuum approach were proposed (Chou and Lee 2009, 2011). These models attempt to investigate morphology and movement mechanisms of debris flow in different flow regimes from a particle physics perspective. Numerical modelings based on continuum approach (Dai et al. 2017, 2020; Cuomo et al. 2019, 2021) discontinue approach (Borykov et al. 2019) and coupled of both, named coupled computational fluid dynamics (Li et al. 2020), were extensively deployed to reveal the mechanism of debris flow and the relevant flow-structure interactions. For example, Cuomo et al. used the smoothed particle hydrodynamics (SPH) method to investigate the propagation pattern of debris when artificial barriers are adopted. Their model predicts a better barrier efficiency against debris flow when the barrier was located immediately at the toe of the slope or at a few meters distance or even in the presence of two barriers (Cuomo et al. 2019). Cuomo et al. simulates a dry granular flow impacting a rigid wall under different geometries and conditions, and found that the presence of liquid phase inside the granular flow is important (Cuomo et al. 2021). Dai et al. also uses a SPH method to simulate the Wenjia and Hongchun gully debris flows, and the peak velocity of the debris flow and the maximum impact force on the check dams are obtained. The sensitivity of viscosity was also evaluated (Dai et al. 2017). The abovementioned studies have successfully proved that the numerical model can be used as a reliable tool in analyzing debris flow

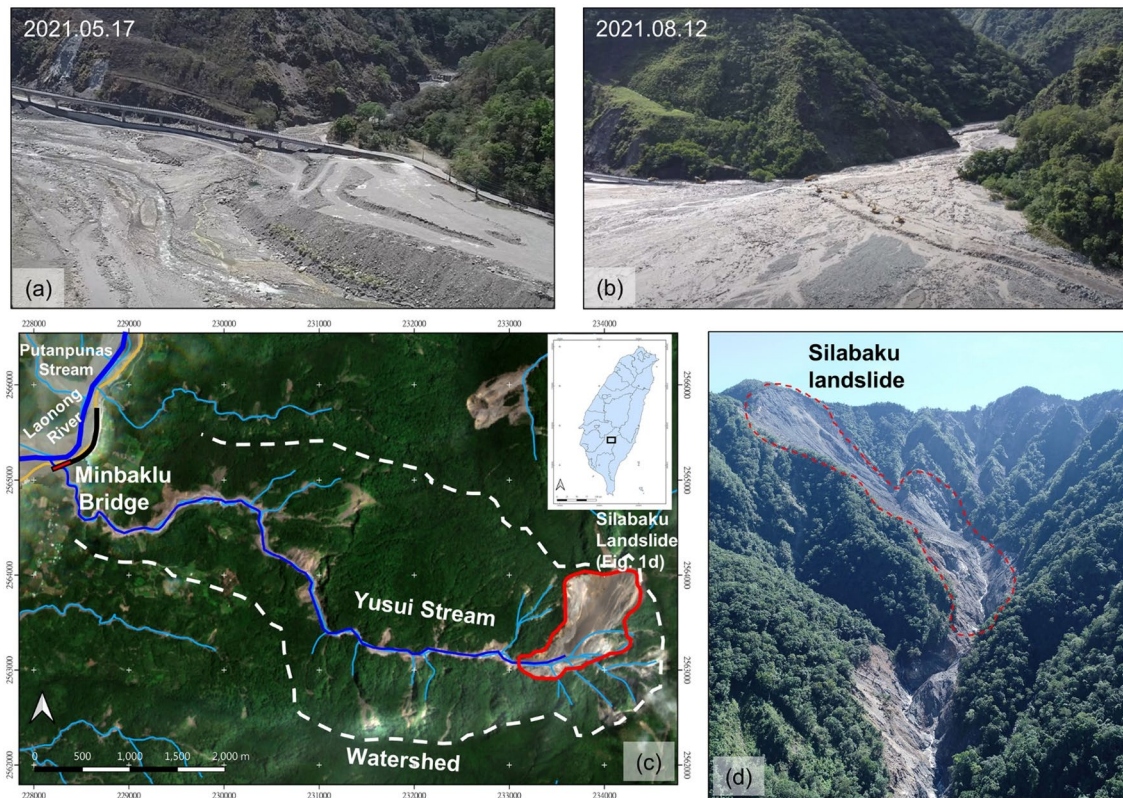


Fig. 1 Overview of the failure event of the Minbaklu Bridge, the debris flow of the Yusui Stream, and the landslide of the Silabaku landslide. **a** The Minbaklu Bridge before the disaster. **b** The Minbaklu

Bridge after the disaster. **c** The watershed of the Yusui Stream. **d** The Silabaku landslide

behavior and its interaction with solid structures. However, a full process of debris flow event from landslide induced flow initiation, through the formation and the collapse of a natural dam, toward massif debris flow run-out simulation and the final flow-bridge interaction, including collision and separation, was not yet seen in the past studies. It is worth mentioning that the process of the Minbaklu Bridge failure is recorded, which provides solid evidence for the following simulation.

To investigate the development process of debris flow and the failure mechanisms of the Minbaklu Bridge, this study conducted a series of analyses, including (1) analyzing the precipitation data, (2) collecting the geological condition, (3) comparing the historical evolution of the landslide, (4) building digital terrain model and performing spatial analysis, and (5) investigating the seismic waveform, to acquire the reasonable disaster timeline. Based on the data, a hybrid model of the discrete element method and depth-averaged model was proposed to simulate the event through three stages: formation of the natural dam, debris flow triggered by dam braking, and bridge collapse due to debris flow. The results obtained can provide comprehensive and objective information to authorities to formulate hazard mitigation strategies and reconstruction projects in the future.

Information of the debris flow event

The Yusui Stream, the object of this research, flows from east to west, and merges with the left side of the Laonong River. The elevation ranges from 600 to 2200 m above sea level. The total area of the watershed is approximately 1,282,000 m² (Fig. 1c). The post-disaster aerial photography showed that the debris material primarily originated from the Silabaku landslide (Yang et al. 2022), which is located upstream of the Yusui Stream (location: 23.170026°N, 120.840611°E; Fig. 1d).

Precipitation

Typhoon Lupit on Aug. 7 was the primary source of precipitation. The typhoon path facing towards the Yusui Stream watershed resulted in heavy rainfall. Figure 3 shows the rainfall time series diagram of the landslides in the upper Yusui Stream. The bar chart reflects the variations of hourly precipitation, and the red line indicates accumulated precipitation. Considerable rain arose at 5–7 a.m. on August 8, 2021. Then, a large-scale landslide (accumulated rainfall of 574 mm) occurred at 9:17 a.m., which was verified by seismic signals. Meanwhile, rainfall intensity gradually slowed. However, the Minbaklu Bridge was destroyed by debris flow at approximately 1:30 p.m.

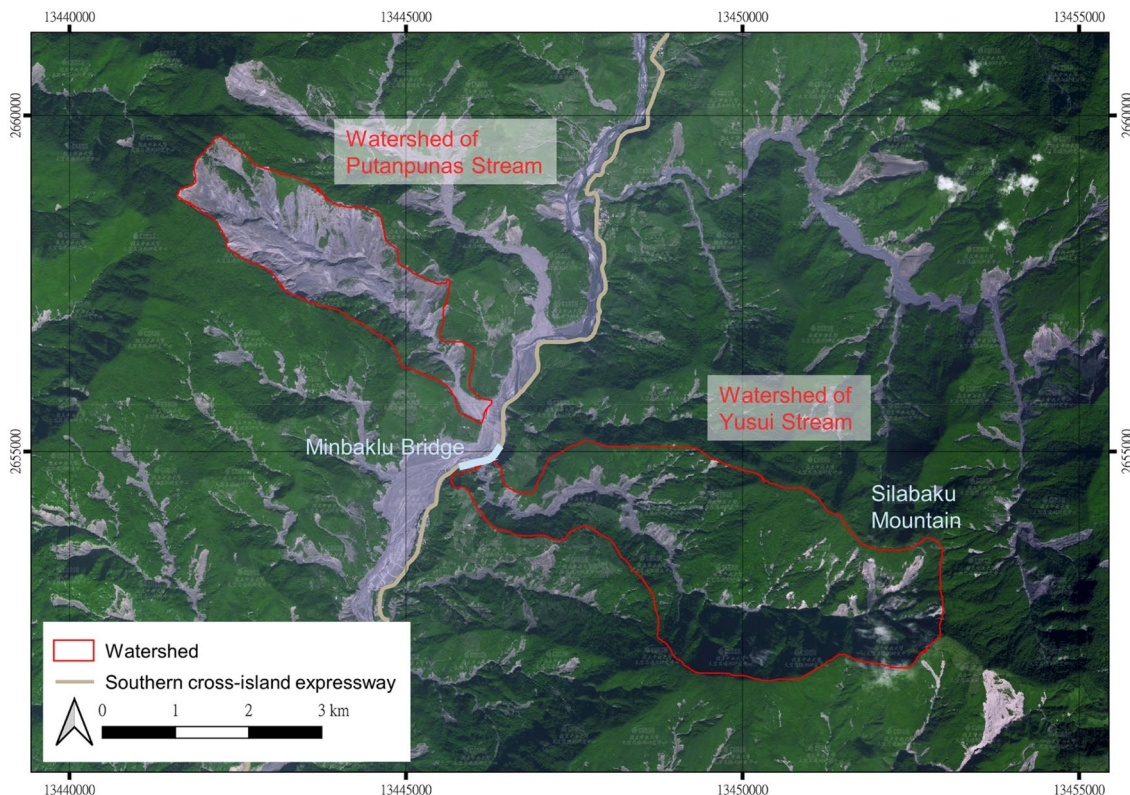


Fig. 2 Overview of the relationship between the Minbaklu Bridge, the Putanpunas Stream, and the Yusui Stream after the 2009 Typhoon Morakot event. The satellite image is provided by Center for Space and Remote Sensing Research (CSRSR), NCU

Geological background

Two geological structures, the Kuaigu and Weichinshi faults, along the northeast-southwest direction, were recognized in the watershed (Fig. 4a). The Kuaigu fault is located upstream, whereas the Weichinshi fault is located in the middle of the watershed, which also forms the boundary between the Pilushan and Chaochou Formations. The Chaochou Formation belongs to the Miocene epoch and is composed of argillite and slate. In contrast, the Pilushan Formation is older, and is composed of argillite, slate, and phyllite. Further, the slate at the source area of Yusui Stream contained ubiquitous and easily

weathered cleavages (Fig. 4b and c). The undesirable mechanical properties of cleavage may result in large-scale landslides and debris flows, which have already been investigated in lots of literature. For example, Weng et al. 2020 obtained the mechanical behavior of slate from Tiangul Creek which belongs to same epoch with Chaochou Formation, and found that water can effectively reduce the strength of slate; on the other hand, lots of historical disasters are reported in this area, such as Lo et al. reported the landslide of the Putanpunas Stream (Lo et al. 2018), and Huang et al. analyzed the relationship between foliation dip direction, downslope direction, and the happenness of landslide in this area (Huang et al. 2016), and Weng et al. investigated the occurrence frequency of landslide in the Lawnon River Basin after the 2009 Typhoon Morakot event found that the incidence of landslides increased significantly (Weng et al. 2011).

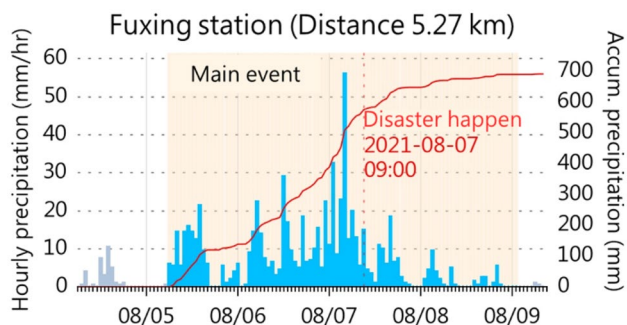


Fig. 3 Rainfall time-series diagram for landslide events at the upstream reach of Yusui Stream

Historical evolution of the source landslide

The Silabaku landslide, a previously occurred large-scale landslide, was the source of debris flow and providing abundant debris. Figure 5 shows the evolution of the Silabaku landslide from the orthoimages of aerial photos and satellite images from 2007 to 2020. In 2007, an unclear lineation along the ridge was developed (Fig. 5a). Thereafter, typhoon Morakot in 2009 caused devastating rainfall and triggered landslides. The landform was clearly exposed following the typhoon event (Fig. 5b), and the failure of the right limb continued to expand. After 10 years, the expansion

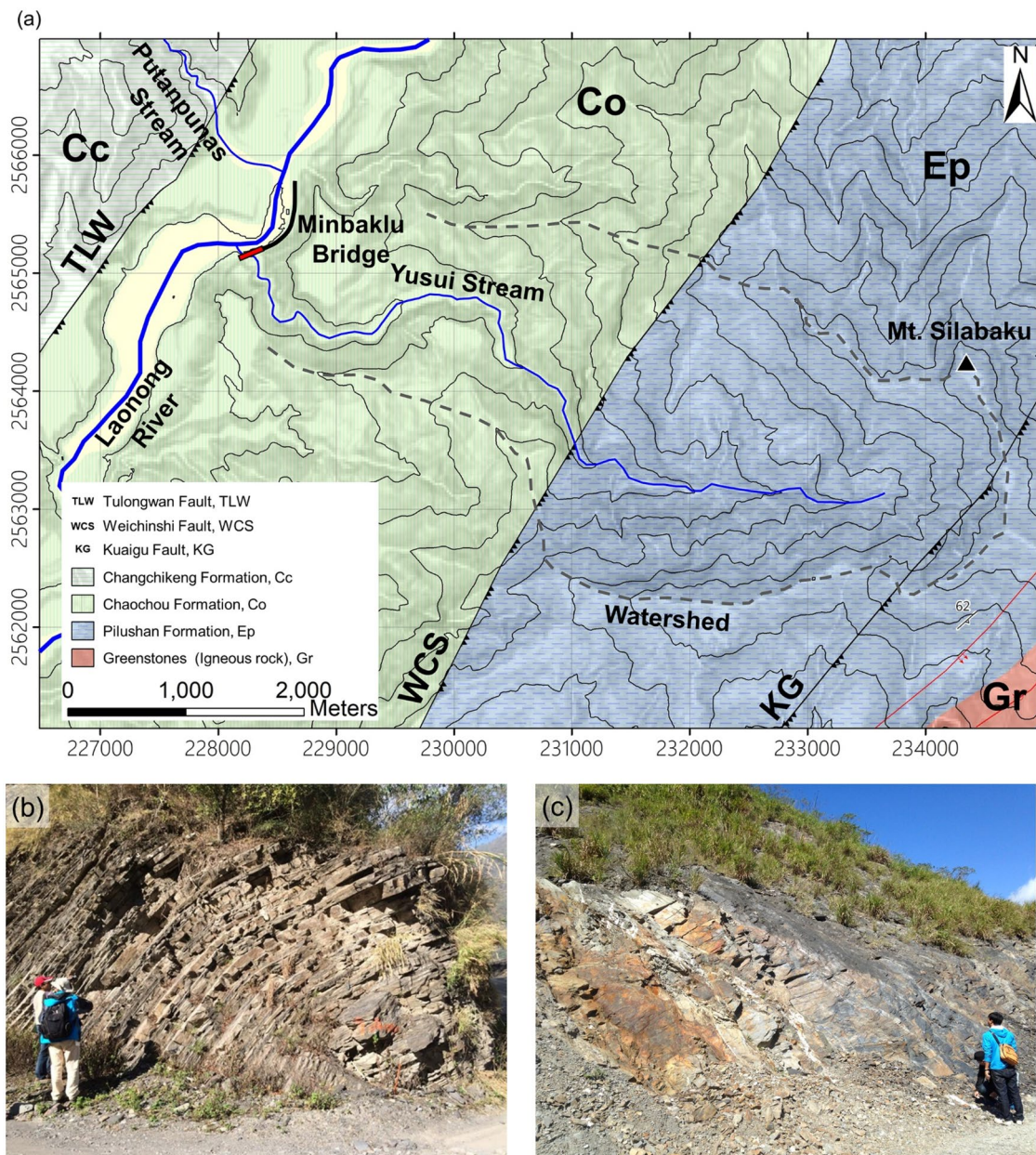


Fig. 4 a Regional geology of the Yusui Stream watershed. Remarks: a: alluvium. Cc: Changchikeng Formation. Co: Chaochou Formation. Ep: Pilushan Formation. Gr: Greenstones (Igneous rock). TLW: Tulong-

wan Fault. WCS: Weichinshi Fault. KG: Kuaigu Fault. b The outcrop picture of Chaochou Formation, film at Yusui Stream, and c Pilushan Formation film at Ali, Pingtung

continued, thereby reflecting that the slope body was weak and unstable (Fig. 5c, d). The prominent scarp extended in 2019, and the displaced mass moved downward. Consequently, the toe failure spread upward and developed a gully. This implies that the structure of the displaced mass fractured with high permeability before the event in August 2021 (Fig. 5e, f).

Spatial analysis of debris flow

To elucidate the landform variations during the debris flow event, the aerial photos obtained from pre-event digital elevation model from high-resolution LiDAR (light detection and ranging) in

2014 and post-event digital surface model from UAV (unmanned aerial vehicle) were compared. Although a difference in vegetation between the digital elevation and digital surface models was observed, most concerned areas (such as river beds, alluvial fans, and landslides) were already exposed. Hence, the calculated terrain difference between the digital elevation and digital surface models was reasonable to warrant further analysis. Figure 6 shows the terrain variations along the Yusui Stream before and after the debris event (warm colors indicate erosion, and cold colors represent deposition). The profile along the stream is plotted in Fig. 7. During this event, the Yusui Stream can be divided into three parts (Fig. 6). The first part is the source area, wherein it is indicated that

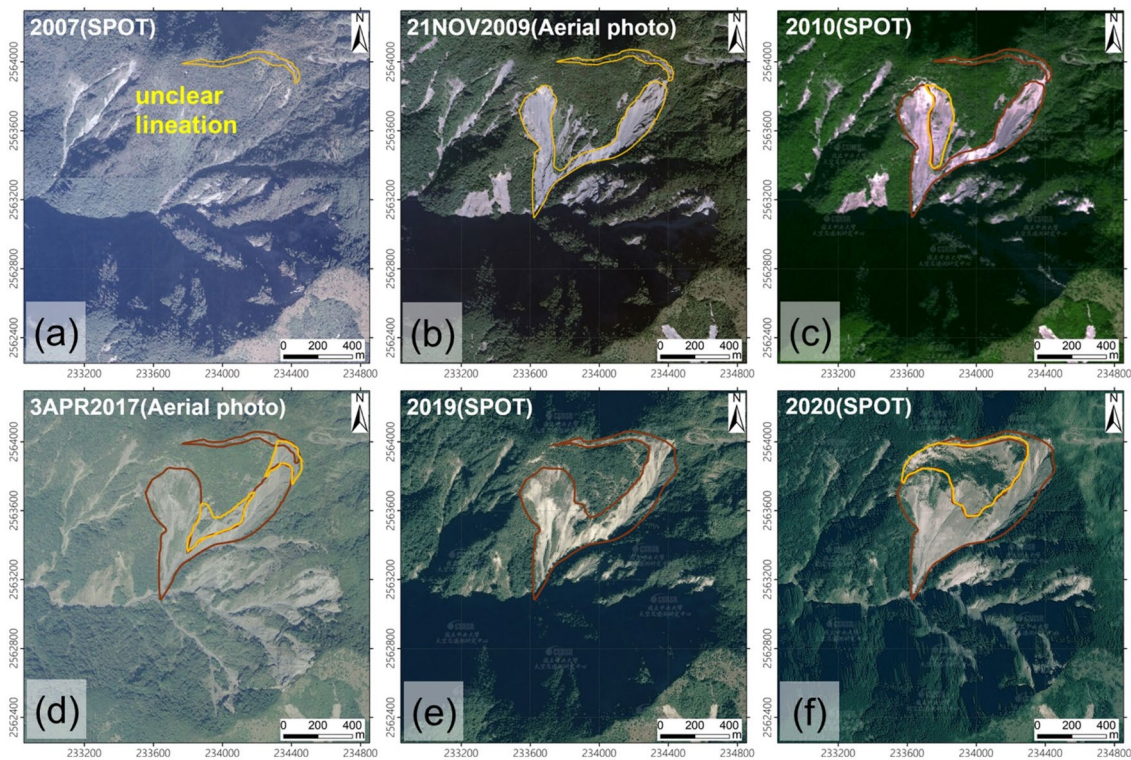


Fig. 5 Evolution of the Silabaku landslide from 2007 to 2020. Brown regions are previously exposed areas and yellow regions are newborn exposed areas compared to the previous image

the Silabaku landslide generated a large amount of debris material, which resulted in the formation of a natural dam that blocked the stream (70 m high; blue area located at the C–C' section in Fig. 7).

The second part is the flow area (Fig. 6). The riverbed was observed to have been deeply eroded by the debris flow (green line in Fig. 7), resulting in the generation of further debris material. The third part is the deposition area. It is obvious that a large amount of material was deposited here and formed an alluvial fan. This deposition impacted the Minbaklu Bridge and finally caused a collapse disaster.

Time series analysis of landslide-induced seismic signals

A seismic analysis of the seismic signals recorded at the nearest station (station code: BNAF) showed that the landslide event started at ~ 09:16:52 (hh:mm:ss, local time) with a duration of ~ 86 s (Fig. 8). The S-transform spectrogram (Chen et al. 2013) for the north–south component at the BNAF station exhibits the dominant frequency of background river noise in the range of 5–10 Hz. The primary erosion area mobilized the collapsed materials, thereby generating a

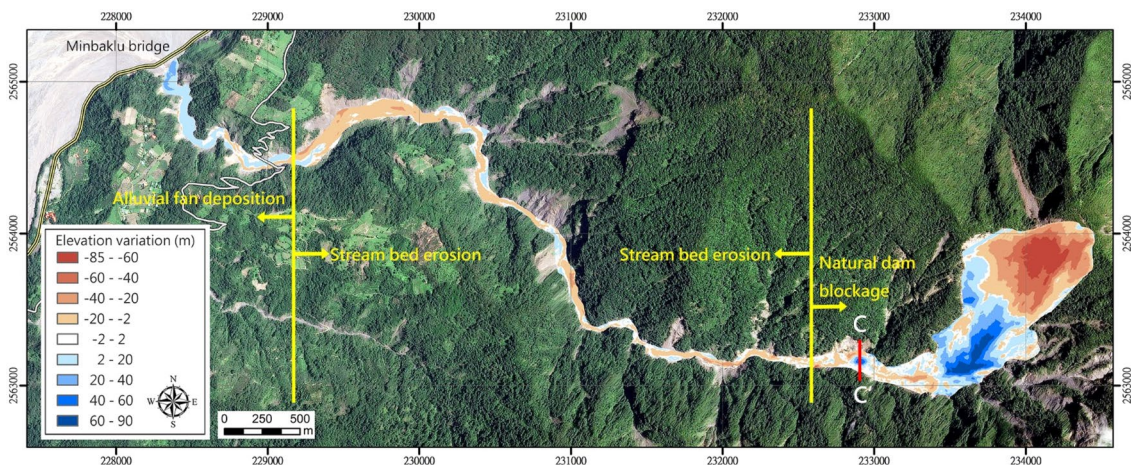
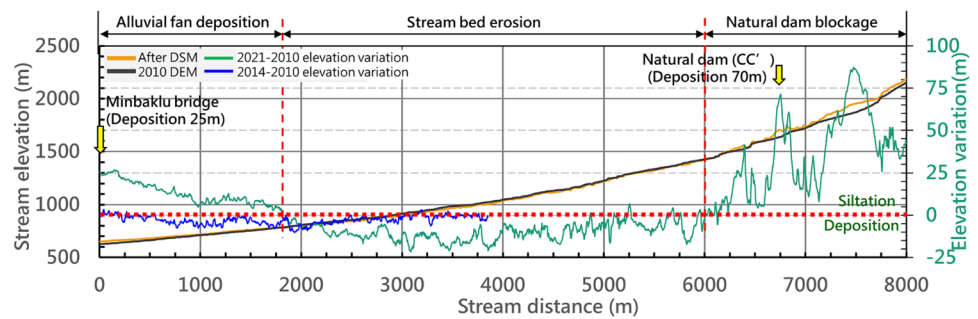


Fig. 6 Terrain difference between pre- and post-event of the Yusui Stream. Warm colors mean erosion and cold colors represent deposition

Fig. 7 Elevation variations between pre- and post-event along the stream



relatively wide frequency band ranging from 0.2 to 30 Hz. Further, signals during the sliding mass deposit stage excited the spectral power below 2 Hz (Fig. 8). Notably, a strong seismic amplitude with a dominant frequency of 0.2–2 Hz can be observed at approximately 09:17:38, which may have corresponded to a sliding mass impacting the topographic barriers and/or stopping shortly in the river channel (rectangle shown in Fig. 8).

Methodology

To investigate the process of debris flow and its impact on the Minbaklu Bridge, a hybrid model combining the depth-averaged model and discrete element method was proposed. The depth-averaged model, which is the RAMMS software (RAPid Mass Movement Simulation) was used to simulate the flow process of the debris flow, including erosion and deposition, and the discrete element method PFC^{3D} software (Particle Flow Code 3 Dimension) was adopted to simulate the damage process of the Minbaklu Bridge under the impact of debris flow.

Depth-averaged model—RAMMS software

The RAMMS two-dimensional numerical simulation program in 3D alpine terrain was developed by the Swiss Federal Institute for Forest, Snow, and Landscape Research (WSL). Its predecessors were the Aval-1D and Aval-2D models developed in 1998–2000. In 2005, the modules were integrated into RAMMS numerical simulation software. This model includes the avalanche model (AV), rockfall (Rockfall), and the debris flow model (DF) module used in this study. RAMMS can directly simulate the phenomenon of debris flow formed by loose geological material sliding into a stream following the occurrence of a landslide. In addition, the block release or hydrological histogram approach can be determined as the basis for the initial setting of landslides based on field data. In addition, RAMMS offers the advantage of simulating dynamic entrainment behavior on a riverbed triggered by debris flow. Further, the RAMMS-DF model uses the Voellmy-Salm rheology model (Voellmy-fluid flow law) as the theoretical basis (Voellmy 1964; Salm 1993), and can

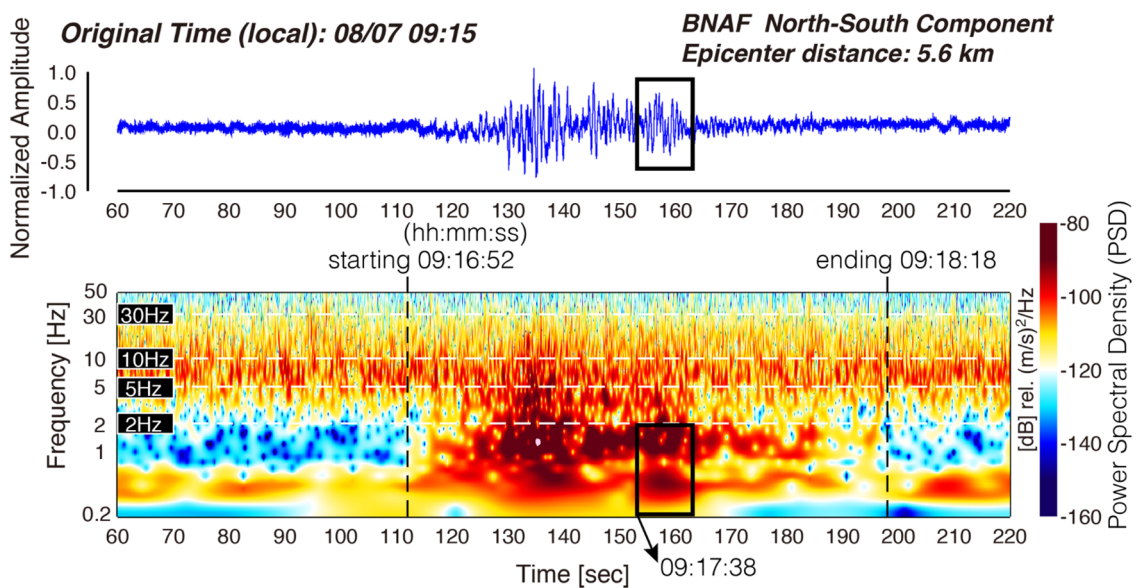


Fig. 8 S-Transform time–frequency map of the East–West component seismic signals at the BNAF station. Vertical dashed lines show the time-points associated with starting and ending of landslide.

Black rectangle indicates the seismic phase corresponding to sliding mass impacting the topographic barriers and/or depositing in the riverbed

describe the sliding behavior of landslides considering the average depth of hydraulics. The mass balance equation of the Voellmy-Salm model is expressed as (Christen et al. 2010; Hussin et al. 2012),

$$\frac{\partial H}{\partial t} + \frac{\partial(HU_x)}{\partial x} + \frac{\partial(HU_y)}{\partial y} = Q(x, y, t) \quad (1)$$

where U_x and U_y represent the speed of the x and y axes, respectively and $Q(x, y, t)$ is the mass source of the bed, or the entrainment rate ($Q > 0$) or deposition rate (deposition rate; $Q < 0$). The depth-averaged momentum balance equation in the x - and y -directions can be expressed as:

$$\frac{\partial(HU_x)}{\partial t} + \frac{\partial\left(c_x HU_x^2 + \frac{g_z k_a H^2}{2}\right)}{\partial x} + \frac{\partial(HU_x U_y)}{\partial y} = S_{gx} - S_{fx} \quad (2)$$

$$\frac{\partial(HU_y)}{\partial t} + \frac{\partial\left(c_y HU_y^2 + \frac{g_z k_a H^2}{2}\right)}{\partial y} + \frac{\partial(HU_x U_y)}{\partial x} = S_{gy} - S_{fy} \quad (3)$$

where c_x and c_y are the shape factors that depend on the terrain DEM; k_a is the earth pressure coefficient; S_{gx} and S_{gy} are the gravitational accelerations in the x and y directions, respectively; S_{fx} and S_{fy} represent the friction terms in the x and y directions, respectively; and $S_f = (S_{f,x}, S_{f,y})^T$. In the Voellmy-Salm rheology, the relationship is expressed as:

$$S_{fx} = nU_x \left[\mu g_z H + \frac{g \|U\|^2}{\xi} \right] \quad (4)$$

$$S_{fy} = nU_y \left[\frac{\mu g_z H + g \|U\|^2}{\xi} \right] \quad (5)$$

The Voellmy-Salm model decomposes the total basal friction coefficient into two parts: the dry-Coulomb friction coefficient (μ) independent of speed and the turbulent friction coefficient (ξ) dependent on speed. The former parameter controls the runout distance of the landslide, whereas the latter affects the movement time of the landslide.

In addition, this division can simultaneously describe the flow behavior of the collapse acceleration and deposition zones and assumes that the shear deformation is concentrated at the end of the bottom flow surface.

Discrete element method—PFC software

The PFC^{3D} was adopted to simulate the interaction between debris flow and engineering structures because of its unique characteristics, including the ability to simulate particle flow, large deformation, and collision interactions. The theory of PFC is based on the dynamic relaxation method and is primarily driven by two equations: the force-displacement law and Newton's second law. Thus, the mechanical behavior of the analysis problem can be obtained through many iterations and this process can be repeated until the simulation is complete. The applicability of the PFC has been proven in several types of research, demonstrating its excellent

capability in investigating discretized problems (Chiu et al. 2015; Lin and Lin 2015; Weng et al. 2019, 2020; Chiu and Weng 2019), particularly in simulating the debris flow problem (Lo et al. 2011).

RAMMS-PFC coupling model

The discrete element method approach has been extensively employed in landslide disciplines to capture phenomena related to large-scale slope instability, such as rock avalanches or debris flows. A generic numerical model that addresses this issue must consider the topography, geological formation, and other factors that stimulate slope instability (weathering, degradation, ground water condition, etc.). Upon triggering of the slope collapse, the detached material moves downward through the valley of the topography and produces a significant run-out distance. However, the aforementioned discrete element method concept cannot be applied to debris flow events in the present study for two reasons. First, the concerned topography is close to the stream estuary and presents a nearly flat landform slope of approximately 5°. The only force driven by gravity is not sufficiently strong to push the balls or even to wash out the bridge deck. Second, the debris flow material was mixed with crushed rock mass and water. The transportation behavior of this type of wet debris is expected to be a fluidized material rather than a solid ball. Therefore, it is necessary to consider the seepage force acting on the ball.

The proposed RAMMS-PFC coupling model is a one-way computational fluid dynamics (CFD) coupling method. The innovation is that the flow field is captured from the RAMMS result rather than a constant field. However, in the coupling process, the debris flow model using RAMMS must be performed prior to the application of the PFC model. Thus, the coordination of the RAMMS meshes and their flow velocity and water pressure were extracted and then imported into the PFC model, which served as reference values for the seepage force calculation. Consequently, the flow velocity can be used to calculate the drag force, \vec{F}_{drag} , which is defined as (Di Felice 1994; Xu and Yu 1997)

$$\vec{F}_{drag} = \frac{1}{2} C_d \rho_f \pi r^2 |\vec{u} - \vec{v}| (\vec{u} - \vec{v}) \varepsilon^{-\chi} \quad (6)$$

where C_d is the drag coefficient (-); ρ_f is the fluid density (kg/m³); r is the ball radius (m), \vec{u} and \vec{v} are the fluid velocity (m/s) and ball velocity (m/s), respectively; and ε is the porosity of the fluid element (-).

The drag coefficient is defined as:

$$C_d = \left(0.63 + \frac{4.8}{\sqrt{R_{ep}}} \right)^2 \quad (7)$$

where R_{ep} is the ball Reynold number.

The empirical coefficient χ is defined as:

$$\chi = 3.7 - 0.65 \exp \left(- \frac{\left(1.5 - \log_{10}^{R_{ep}} \right)^2}{2} \right) \quad (8)$$

The ball Reynold number is:

$$R_{ep} = \frac{2\rho_f r |\vec{u} - \vec{v}|}{\mu_f} \quad (9)$$

where μ_f is the dynamic fluid viscosity (Pa s).

The water pressure extracted from the RAMMS can be used to calculate the force due to the fluid pressure gradient \vec{F}_{pgrad} , which is obtained by the following equation:

$$\vec{F}_{pgrad} = \frac{4}{3} \pi r^3 \nabla p \quad (10)$$

where ∇p is the pressure gradient (Pa/m).

Following the determination of the above two forces, \vec{F}_{drag} and \vec{F}_{pgrad} , the equivalent seepage force (\vec{F}_{sf}) is then calculated using the following equation:

$$\vec{F}_{sf} = \vec{F}_{drag} + \vec{F}_{pgrad} \quad (11)$$

Thereafter, the seepage force obtained from Eq. (11) is applied at the ball centroid and coupled with Cundall's contact force works in the force–displacement iteration (Fig. 9). Subsequently, during the PFC simulation, the corresponding flow velocity and water pressure captured from the RAMMS were automatically updated according to the PFC time advancement, and then, the applied forces on each PFC ball are refreshed based on its location.

Model settings of Yusui Stream event simulation

According to the debris flow event description in “Information of the debris flow event,” the proposed hybrid model was used to elucidate the event through three stages: formation of the natural dam, debris flow triggered by dam braking, and bridge collapse owing to debris flow. Details of the simulation process are described below.

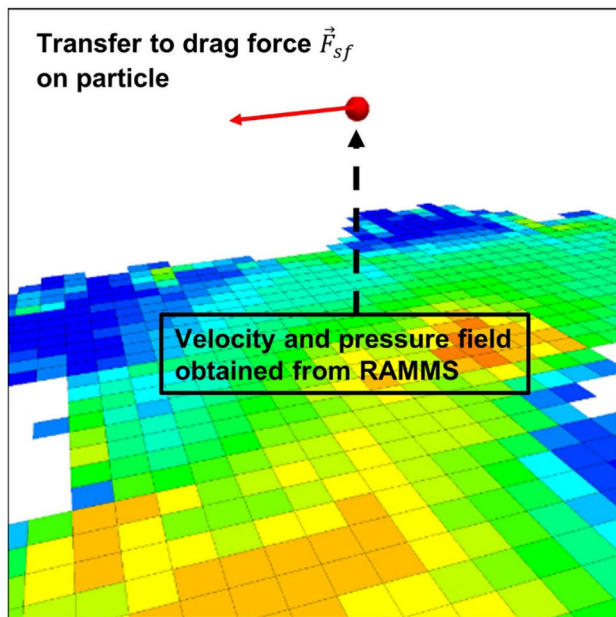


Fig. 9 Schematic diagram of RAMMS-PFC coupling

Forming of the natural dam

In the simulation of natural dam formation, we used the engineering data and on-site survey data from the SWCB and Directorate General of Highways (DGH) before and after the disaster. The required parameters for the simulation include the unit weight, dry frictional coefficient, viscous-turbulent coefficient, and landslide area, averaged sliding depth, which is listed in Table 1. The mechanical parameters are obtained from the laboratory reports of the previous works. At the same time, the landslide area and depth are taken from the DEM (2014, 2021) and satellite image analysis (Google Earth, Planet Lab) before and after the event.

At this stage, the simulation assessed whether a natural dam was formed in the upstream section of Yusui Stream following a large-scale landslide. After the occurrence of the landslide, many landslide materials were gradually deposited dynamically to reach a final stable state, and the influence of water flow was not considered at this stage. Further, the dynamic parameters of the RAMMS simulation of debris flow, such as flow depth and velocity, were output to the PFC model at the check dam in the downstream section.

Debris flow

Following the formation of the natural dam, the successive flow caused its destruction and breakage. In the second stage of the simulation, following the dam breakage, a large amount of geomaterial was mixed with surface runoff, which formed a debris flow. According to the real-time video at the downstream reach and in situ observations, in terms of material composition conditions, the debris flow was a typical dense mud-sand mixture. The parameters for the simulation in the second stage are listed in Table 2. The detailed input parameters were selected and considered to reflect the reality as much as possible. Based on the RAMMS user's manual, the reasonable range of the dynamic viscous turbulent coefficient (ξ) for mud-like debris flow is approximately 200–1000 m/s². In addition, Schraml et al. (2015) summarized the debris flow and landslide events around the world and classified them into three levels according to the landslide volume. Medium-scale volume ($V < 106 \text{ m}^3$) should have a debris flow value of approximately 200–350 m/s², and for large-scale mass ($V > 108 \text{ m}^3$) debris flow, the ξ value is distributed between 200 and 1000 m/s². The estimated volume of the debris flow in the disaster considered in this study was approximately $1.76 \times 10^7 \text{ m}^3$; thus, the regression value of

Table 1 The required parameters for RAMMS simulation on the natural dam formation

Parameter	Value
Landslide area, A (m ²)	572,250
Landslide averaged depth, h (m)	45.0
Landslide volume, V (m ³)	34,614,802
Density, ρ (kg/m ³)	2670
Frictional coefficient, μ	0.4 (22°)
Viscous-turbulent coefficient, ξ (m/s ²)	200

Table 2 The input parameters for RAMMS simulation of debris-flow process

Parameter	Value
Landslide area, A (m^2)	353,625
Landslide averaged depth, h (m)	26.1
Landslide volume, V (m^3)	17,635,820
Density, ρ (kg/m^3)	2200
Frictional coefficient, μ	0.11 (6.1°)
Viscous-turbulent coefficient, ξ (m/s^2)	500
Erosion rate (m/s)*	0.025
Potential erosion depth (m/per kPa)*	0.10
Critical shear stress (kPa)*	1.00
Max erosion depth (m)	5.00

*Reference: Schürch et al. (2011) and Frank et al. (2015)

500 m/s^2 was considered as the input value for ξ . In other words, for the Coulomb friction coefficient (μ) of the debris flow material, the measured value of the slope gradient in the downstream alluvial fan was 6.1° ($\mu = 0.11$). The friction coefficients for Voellmy-Salm rheology were calibrated using the 3D terrain landform. Further, RAMMS can determine the stream bed as an erosion zone (entrainment effect).

Most conventional models have not considered the erosion of the streambed; thus, the inflow of the debris flow simulation is equal to the outflow. However, this result is not consistent with the actual phenomenon. In reality, during debris flow movement, erosion occurs at the bottom of the stream when the momentum of the moving body is more significant than a specific critical value. As a matter of fact, the erosion rate and critical shear stress control the scouring depth of the sediment material. Very few values are available from the field survey, so RAMMS proposed an invariant value based on the work published by Berger et al. (2011). The maximum erosion depth in the entrainment model is a function of the channel-bed shear stress and the vertical erosion rate. This study pre-simulated the topographic differences at estuarine alluvial fans between the pre- and post-event to obtain reasonable maximum erosion depth. Finally, we got a potential maximum erosion depth (~ 5 m). In addition to using the post-event terrain for calibrating relevant parameters, this study also referred to the recommendations in the literature (Berger et al. 2011; Schürch et al. 2011; Frank et al. 2015, 2017).

Parameter sensitivity analysis is a procedure for evaluating the influence of parameters on numerical simulation results and is particularly useful for simulations with no parametric basis. This study clarifies the following conclusions based on previous cases of RAMMS analysis and literature review (Schraml et al. 2015; Lee et al. 2016; Abraham et al. 2022). Meanwhile, under the condition that the critical parameters of the simulation input are primarily established, this study did not perform additional sensitivity analysis for the time being. (1) If the parameter values are changed by plus or minus 25%, the final landforms of landslide and debris flow

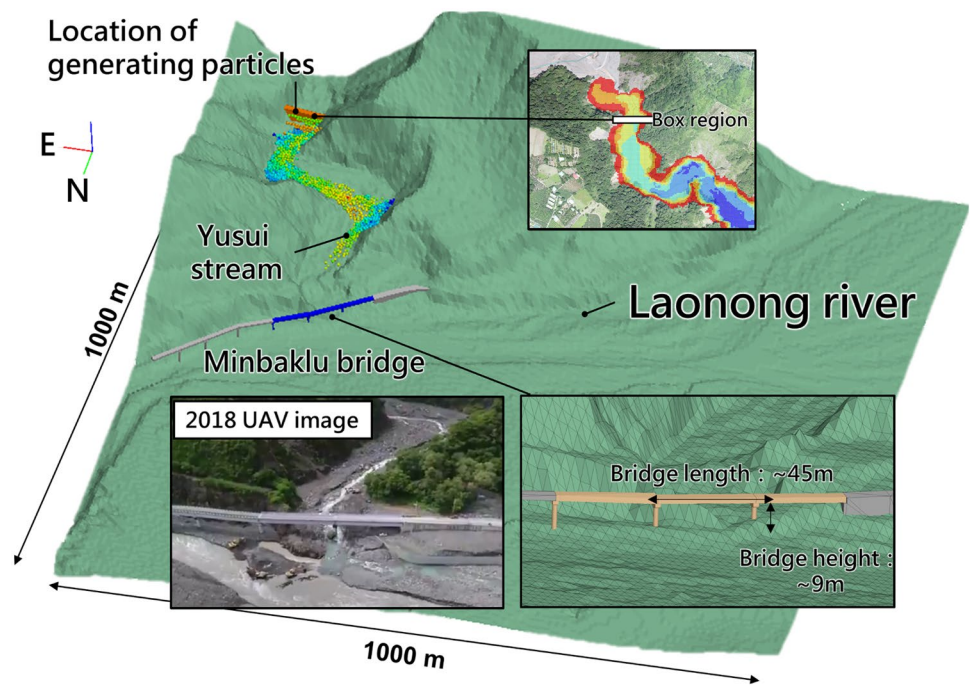
simulations are highly related to the friction coefficient and less affected by the coefficient of viscous turbulence. (2) The numerical simulation results are more consistent with the actual disaster if the input parameters are obtained by back-analysis using the topographic features measured in the field after the event. For example, the superelevation and flow velocity at curved channels can be used to calibrate the viscous turbulent coefficient. Still, such observations are not available for streams in some remote areas, and we suggest that this be considered in the future. The RAMMS simulation termination time is defined as the instantaneous momentum of any step in the simulation, which is less than 5% of the maximum momentum. When the calculation is stopped, it is regarded as the end of the debris flow process.

Bridge collapse

Figure 10 shows the PFC model to simulate the bridge collapse and the development of the alluvial fan. The terrain of the stream is composed of a set of triangulated wall elements, which were constructed employing the latest 1 m LiDAR DEM, and was simplified to a 5-m resolution to improve calculation efficiency. The wall elements are rigid. The model size is 1000 m \times 1000 m, and the resolution of the terrain is 5 m \times 5 m, which means there are 200 \times 200 grid points to form the terrain. The model size is much larger than the influence area of the debris flow deposition; the particles will not overflow out of the model.

The failure of the Minbaklu Bridge was the main disaster in this debris event. The bridge in the simulation included the deck, pillar, foundation, and abutment, which were established from the original engineering blueprints (Fig. 10). The rigid block element (rblock) was adopted to simulate the geometry and properties of the bridge. The rigid block is a convex polyhedron that can interact with balls and provide a better means to simulate a structure with a smooth surface. However, a rigid block is unbreakable. According to the in situ video, the bridge is washed away completely without breakage, and thus, a rigid block can be used to appropriately simulate the bridge. Also, the post-disaster images and videos show that the abutment, foundation, and pillar of the bridge remained undamaged; therefore, those parts in the simulation were fixed to accelerate the calculation. Further, the friction coefficient between rigid blocks was set as 1.0 to reflect the influence of the connections between the pillar and deck. To simulate streaming debris in the PFC model, a specific box region was assigned to the last check dam of the Yusui Stream (Fig. 10). The box was filled with balls (radius ranging from 1.66 to 2.08 m, and average radius of approximately 1.87 m), with the locations also being recorded. Subsequently, the box was removed, and the recorded balls were generated repeatedly to simulate the debris material. The generated balls were assigned an initial velocity toward the downstream, and thus, they flowed into the stream rather than remaining in the box region. The initial velocity was obtained from the RAMMS result, which was approximately 7 m/s. When the balls flowed into the stream, the RAMMS-PFC coupling process applied seepage force onto the balls, causing them to flow downstream and accumulate at the estuary of Yusui Stream. The linear contact model describes the contact behavior between different entities, that is, ball-ball, ball-wall, ball-rigid block, and rigid block-wall. In this study, we simplified the required parameter sets for two reasons. First, the model is

Fig. 10 PFC model layout



aimed at reproducing the debris flow movement through a stream channel; therefore, the Coulomb-slip shear strength (i.e., friction angle) has minimal impact on debris flow material residing in the stream channel. However, the repose angle in the deposition zone is affected by the friction angle, and thus, considering the in situ repose angle observation (approximately 6°), the adopted friction coefficient in the PFC model was set to 0.11 in PFC model. Second, the interaction between debris flow (balls) and bridge (rblock) are a major concern, wherein the dominant factor is the kinetic energy produced by the balls (i.e., mass and velocity of balls). In addition, the influence of stiffness was minimal in this study. Thus, the input stiffness must be sufficiently high to prevent an excessively large interpenetration at the contact. Consequently, the energy is dissipated through the normal and shear dashpot components assigned to each contact. The adopted damping coefficients and other contact properties are listed in Table 3.

Results and discussion

Validation of the natural dam formation

Building upon the numerical simulation program described in “Forming of the natural dam,” this section discusses the process

of formation a natural dam following the occurrence of the large-scale landslide of the Yusui Stream and verifies it employing 3D topography after the slope failure. According to the RAMMS simulation results, approximately 80 s passed from the collapse to the formation of a natural dam. Figure 11 shows the digital terrain model at the upstream reach of the Yusui Stream before and after large-scale landslides. The main landslide volume was deposited on the stream bed between the toe of the main landslide area and the first tributary of the stream. Compared with the seismic signal measured from the landslide (Fig. 8), it took about 90 s from collapse (erosion stage) to deposition (accumulation stage). The characteristics in RAMMS simulation were consistent with the seismic waveform in the time series. The results preliminarily proved that the landslide volume blocks the stream section in the upstream stream after landslide occurrence and generated a new landslide dam. Further, as shown in Fig. 12, we observed an evident V-shaped dam deposition at the first tributary confluence point on the right bank compared to the post-landslide topography (cross-sectional profile C–C’ in Fig. 11).

However, the large-scale landslide volume of the upper reach moved to the first change point of the Yusui Stream and stopped, thereby forming a natural dam that blocked the upstream stream

Table 3 Adopted contact parameters for PFC model

	Elastic modulus (Pa)	Stiffness ratio	Friction coefficient	Normal damping	Shear damping
ball-ball	10^6	2.5	0.11	0.2	0.01
ball-wall	10^7	2.5	0.11	0.2	0.01
ball-rblock	10^8	2.5	0.11	0	0
rblock-wall	10^8	2.5	1.0	0	0
rblock-rblock	10^8	2.5	1.0	0	0

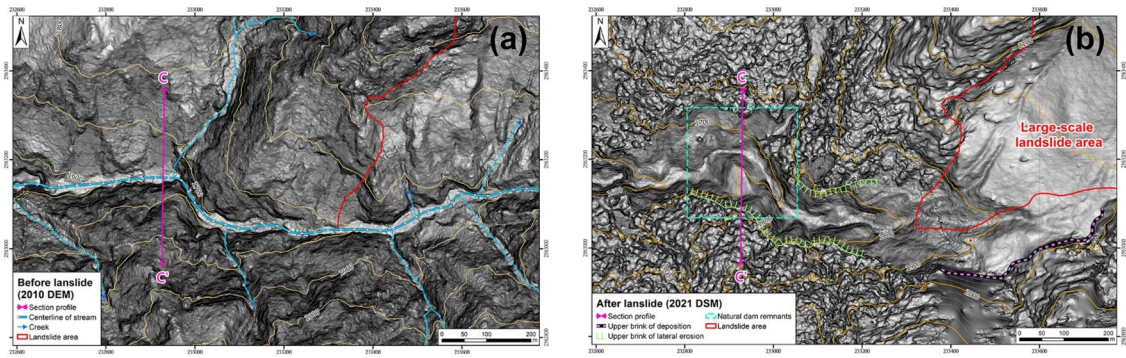


Fig. 11 Digital terrain model at the upstream reach of Yusui Stream (a) before and (b) after large-scale landslides. The blue frame are the location of Fig. 12

channel. The depth of deposition varied from 60 to 80 m (Fig. 12a, b and c). Later, owing to the erosion and overflow of the northern gully, the natural dam was broken, and excessive amount of gravel and soil rushed downstream and subsequently transformed into a debris flow, the remaining materials of natural dam can be founded in Fig. 12d.

The RAMMS simulation results (Fig. 13) (Movie 2) show that when the landslide occurred, the collapsed material of the upper reaches of the Yusui Stream at the right bank tributary stopped

(profile C–C'), and the final deposition height of colluvium could reach 80–120 m. For further comparison, the RAMMS was used to simulate the height of the natural dam located in profile C–C', which is approximately 74 m when 80 s after the occurrence of the landslide process. This result is consistent with post-event topographic analysis and seismic signal measurements. Thus, it is preliminarily verified that a temporary barrier dam was generated in the Yusui Stream during the early landslide stage. From a topographical perspective, following the occurrence of a large-scale

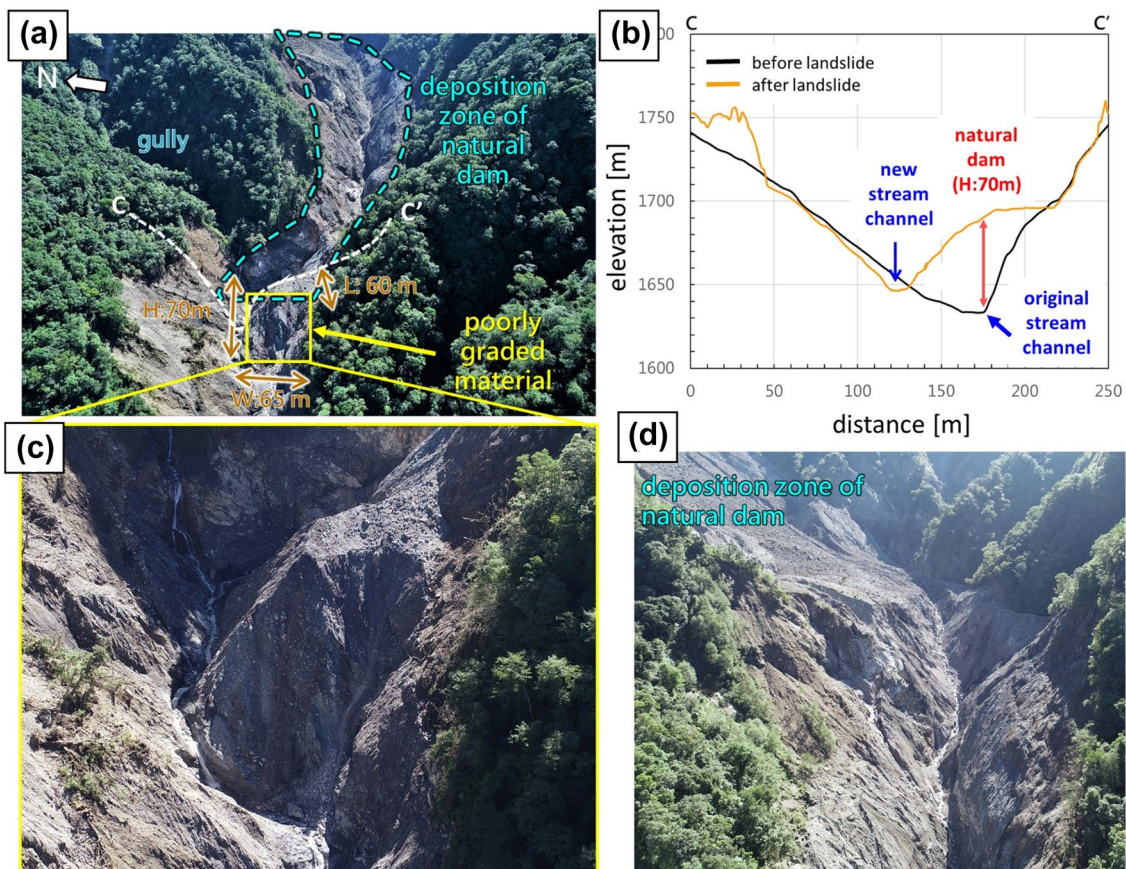
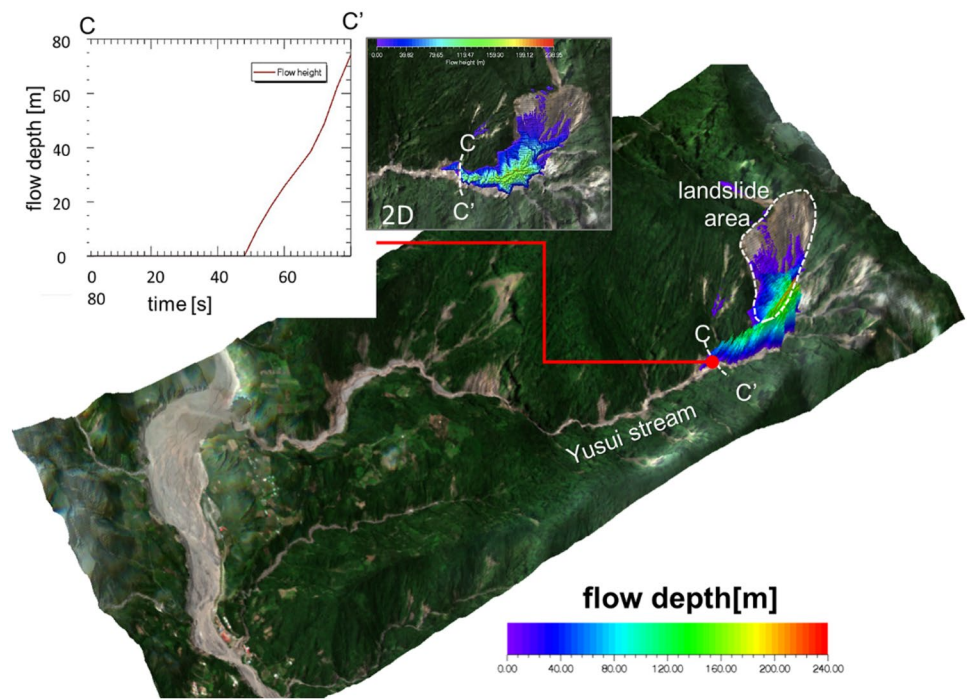


Fig. 12 Terrain feature of the natural dam and cross-sectional profile

Fig. 13 RAMMS simulation result of natural dam formation (For enhancing the visual effect, the 3D simulation depth map presents the deposition depth twice as much as the actual one)



landslide, if the stream is turned or narrowed, the probability of creating a natural dam is significantly increased.

Debris flow transportation process

Natural dam breaking after the occurrence of the large-scale landslide, combined with abundant rainfall and colluvium, provided conditions conducive to triggering debris flows. Considering the simulation parameters discussed in “Debris flow,” Fig. 14a–f shows the RAMMS simulation flow process from the start of the debris flow to the formation of an alluvial fan at the confluence (Laonong River) (Movie 3). In the upstream section, the flow depth of the debris flow can be observed to have increased with decrease in the width of the Yusui Stream (Fig. 14b and c). According to the simulation results, the debris flow simulated by RAMMS reached the Minbaklu bridge at the confluence in approximately 590 s (Fig. 14e) and the transportation time for the entire debris flow to stop was approximately 820 s (Fig. 14f). From the kinematics perspective (Fig. 15; the red-line is the profile X-X'), the maximum flow velocity of the whole debris flow event was 20.1, 18.3, and 10.2 m/s in the upper, middle, and downstream, respectively. The velocity distribution results indicate that the upstream section of the Yusui Stream is straight and has a significant slope gradient and subsequently, the flow velocity of the debris flow gradually slowed down in the middle reaches because of the increase in meandering and the widening channel.

Meanwhile, in the downstream control section (data output for PFC simulation) (Fig. 16), the check dam blocked the debris flow, and the flow velocity dropped within 2–8 m/s. Because it was an obvious object to identify, it was selected as the cut-off point between RAMMS and PFC. Returning to the landform variation, the terraces left by many early debris flow events are located in the middle and lower reaches of the Yusui Stream. Moreover, the

numerical simulation results also verify a more apparent lateral overflow phenomenon in the downstream section after aerial photography after the event. The RAMMS::DF model can simulate the entrainment effect of debris flow on the channel bed. Figure 16 shows the distribution map of the erosion depth of the stream bed after the debris-flow event.

During the debris flow movement, the lateral circulation of the unsaturated-coarse surface layer at the front caused an outward spreading phenomenon. The erosion of the hot zone by the debris flow primarily occurred in the middle section of the stream bed. Overall, the erosion primarily occurred on the centerline of the stream channel (3.0–5.2 m), and its depth decreased gradually (1.5–3.1 m) as it progressed to both sides of the stream channel. On evaluating the entrainment model (eroded bed), the final volume of the debris flow, in this case, was determined to have increased by 11% compared to the fixed bed model. As a result of such analysis, the eroded bed simulation can effectively reflect the outflow volume and potential deposition area of debris flow while assessing the possible influenced area more accurately. Thus, with respect to the wide-range sediment transportation simulation, the RAMMS model can completely and efficiently reproduce the process of landslide transformation to debris flow. Moreover, compared with other numerical models, RAMMS is suitable for disaster prediction and influenced area assessment on a catchment scale.

Debris flow-structure interaction process

Before presenting the debris flow-structure interaction result, the necessity of the RAMMS-PFC coupling model must first be revealed. Figure 17 illustrates the ball movement trend between the RAMMS-PFC coupling model (with seepage force) and the PFC-only model (without seepage force). The initial velocity was accounted for in both models, whereas an additional seepage

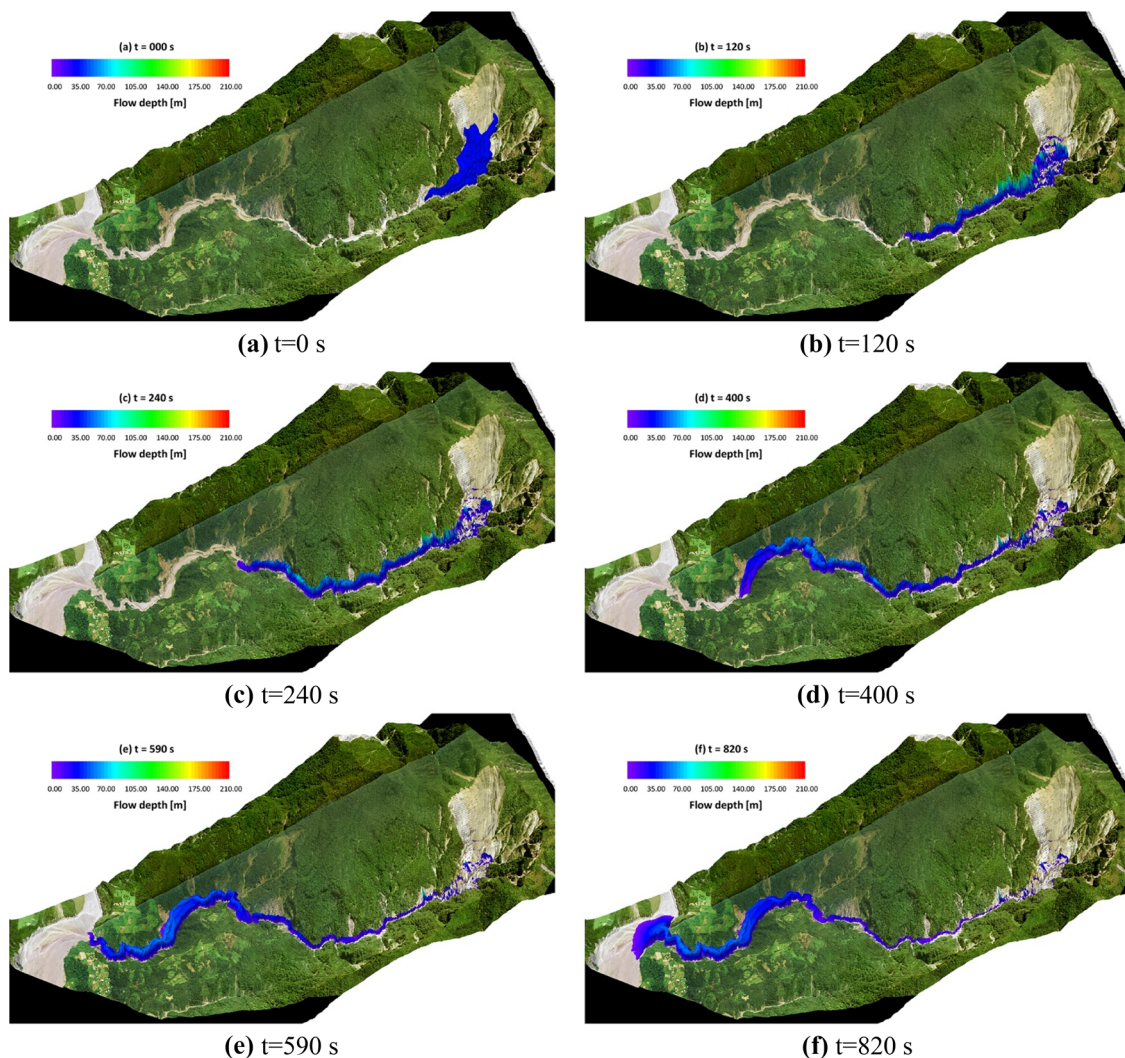


Fig. 14 The RAMMS simulation result of flow depth for debris flow (for enhancing the visual effect, the 3D simulation depth map presents the deposition depth twice as much as the actual one). **a** $t=0$ s. **b** $t=120$ s. **c** $t=240$ s. **d** $t=400$ s. **e** $t=590$ s. **f** $t=820$ s

force, based on the CFD concept, was added to each ball centroid in the case of the RAMMS-PFC coupling model. The results clearly reveal that if the seepage force is neglected, it results in slower debris movement, and the balls are seriously clogged when passing through the first stream turning. In contrast, the RAMMS-PFC coupling model exhibited a more fluent ball movement trend, where the ball velocity contour was fairly synchronized with those calculated in RAMMS. Thus, the above comparisons demonstrate that the proposed coupling model is capable of producing a debris flow-like behavior, even for a topography of nearly flat landform and with certain turning points. Thus, in the subsequent discussion, only the results obtained employing the RAMMS-PFC coupling model are presented.

During the simulation, we monitored the vertical and horizontal contact forces related to the bridge decks. As shown in Fig. 18a, the vertical force represents the vertical reaction force between the pile cap and deck, whereas the horizontal force is the sum of the horizontal contact force (x and y components) between the bridge

deck and balls. Based on the simulation results of the contact force acting on the bridge deck and the bridge displacement history (Fig. 18), the flow-structure interaction can be divided into three stages. First, the generated balls flow through the stream channel and accumulate progressively in the deposition area. During this period, the vertical and horizontal forces of bridge deck D1 (colored red in Fig. 18b) remain unchanged. Here, the initial vertical force of 1.7 MN presented in Fig. 18a denotes the weight of deck D1 and this vertical force also represents the shear strength of the deck according to the Coulomb slip criterion. Subsequently, the balls continuously flowed into the deposition area and their consequent deposition resulted in a back clog toward the bridge. Moreover, certain ball-rblock contacts were detected at the bridge deck (Fig. 18d) when the deposition volume reached $6.2 \times 10^4 \text{ m}^3$ implying that the deposited material was sufficiently thick to start colliding with the deck. Thereafter, we observed a progressive increase in the horizontal force. However, the vertical force diminished during the same period, which may be because certain

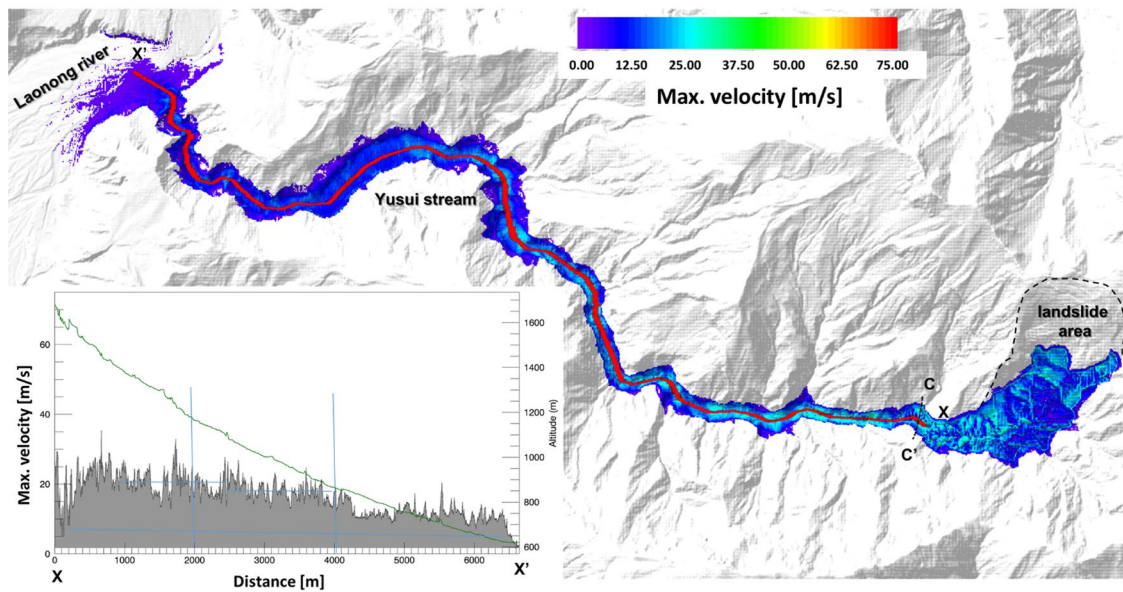


Fig. 15 The RAMMS simulation result of flow velocity for debris flow from natural dam to alluvial fan (profile X-X')

balls hit the deck bottom face, resulting in an uplift force, thereby reducing the vertical force. These uplift forces stimulate the wash-out of the deck. Finally, the debris flow attained the height of the deck top face, and certain balls even flowed over the deck from the top side (Fig. 18e) (Movie 4). Consequently, the bridge deck was pushed out at a deposition volume of $8.2 \times 10^4 \text{ m}^3$. Simultaneously, as the horizontal force increased and was greater than the friction

resistance, the displacement on deck D1 increased. Moreover, the deck push-out of D1 and D2 occurred almost simultaneously, as was captured in the actual situation (Fig. 18g).

In general, strong rainfall-induced debris flow is accompanied by the formation of an alluvial fan at the channel outlet, which was observed in the Yusui Stream event. According to the data provided by SWCB, the deposited volume during the event was estimated to

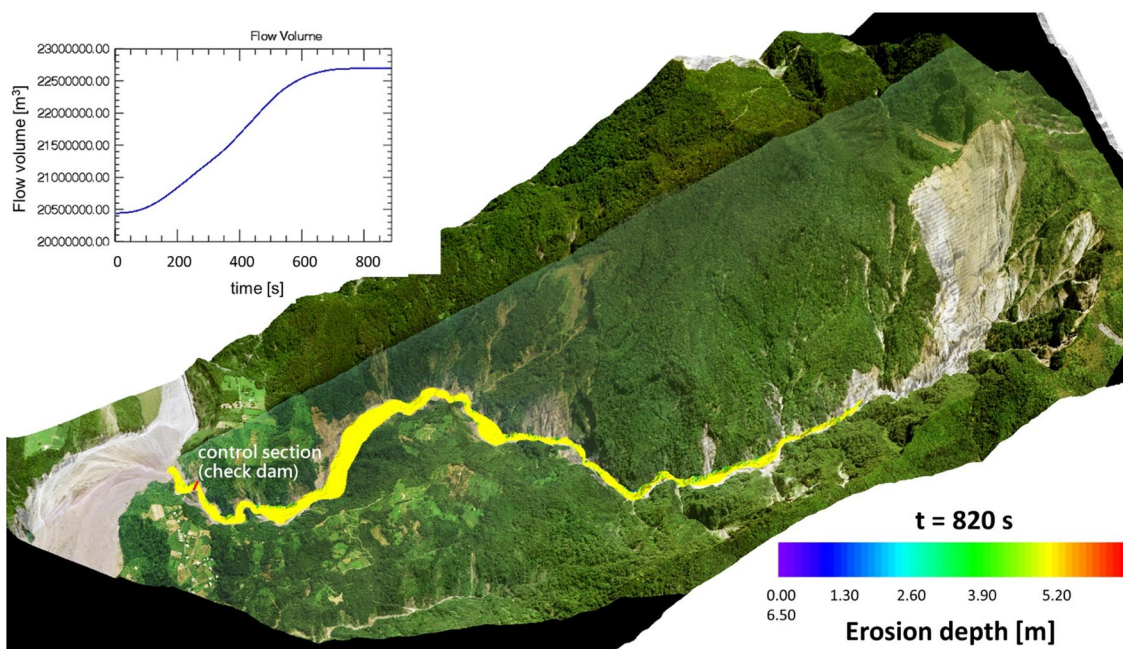


Fig. 16 The RAMMS simulation result of erosion depth for debris flow in Yusui Stream

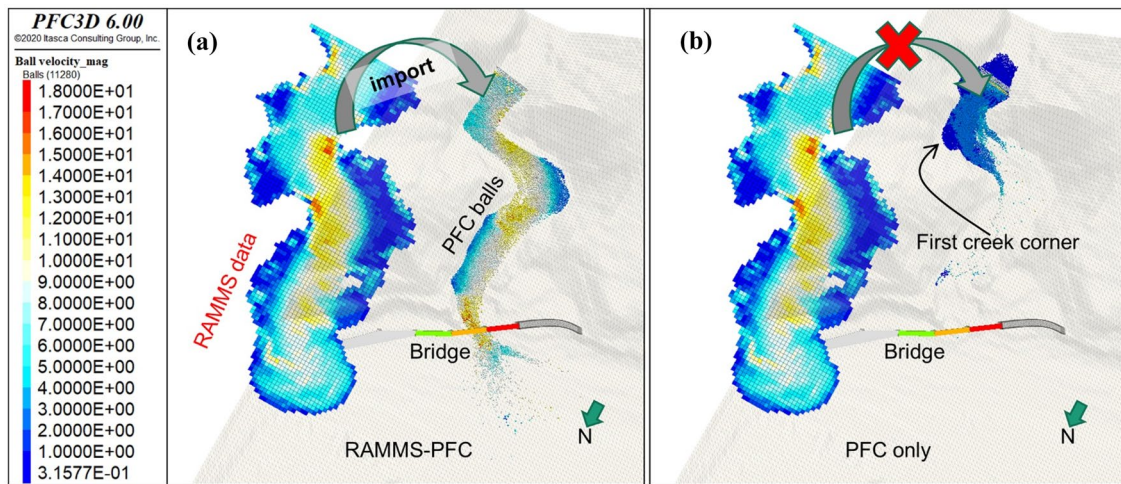


Fig. 17 Ball advancement trend using different approach: **a** RAMMS-PFC coupling and **b** PFC only. The color bar represents velocity contour in m/s

be in the range of 2.5–3 million m³. Thus, the upper bound (3 million m³) was used as an end condition for the PFC simulation; that is, the simulation was terminated when the cumulated ball volume in the deposition zone exceeded the prescribed target value. Figure 19 shows the evolution of alluvial fan formation predicted by the PFC model (Movie 5). The generated balls continuously flowed into the deposition zone and spread freely to fan out in the Laonong River. In addition, a comparable repose angle of the deposited material was determined between the PFC model (5.7°) and the observation data (6°). However, the influence of the main stream (i.e., Laonong River) was not considered in the simulation, and thus, the actual fan shape was ultimately affected by the flow erosion with the edge of the fan being trimmed by the main stream and then elongated along the Laonong River. Therefore, the simulated fan shape was not compared with the actual fan shape in this study, but only verified considering the repose angle.

Figure 20 compares the deposition height between the model and DSM data along a predefined profile (Fig. 20a). The modeling profile is somewhat consistent with the measured profile. Moreover, the apex predicted by the PFC model was found to be very close to the location of the bridge with a thickness of 28 m, similar to that measured from the post-DSM data (approximately 26 m).

Discussion

In the debris flow-structure interaction analysis, the debris flow was simulated using balls in the PFC. Therefore, the gradation of the ball is a major concern. The actual debris was composed of water, mud, sand, gravel, etc., and the ball size varied widely. However, in the PFC, simulating a considerable number of balls is a challenge owing to the limitation of computing ability. In this simulation, the ratio of the maximum to minimum ball radius was approximately 1.25, while

the average radius was approximately 1.87 m, which is quite contrasting to the in situ situation. However, the behavior of the debris flow can still be reproduced because the balls in this study no longer only acted like “balls” such as rock or gravel. Herein, ball movement can be regarded as the impact of debris flow. If the ball number is sufficiently large and its size is sufficiently small, the force exerted on the bridge because of the balls can be treated as a continuous force, which is similar to the force of the debris flow. Therefore, the sizes of the simulated balls are not necessarily consistent with the actual ones. In fact, the determination of ball size is highly related to the height of the bridge deck (approximately 10 m) and computing resources in this study. Moreover, the distance between the bridge deck and the river bed should be sufficiently large to allow at least three balls to move through and thus to consider the computing efficiency, the number of balls was approximately 110,000, requiring approximately 80 h to complete the computation.

In the present study, we demonstrated the failure process of the Minbaklu bridge, from initial collision to fully bridge deck washed out by the massive debris flow mobilization. By analyzing the post DSM data together with the RAMMS results, we found out that only a limited portion of debris material (roughly 3×10^6 m³) was deposited on the Laonong River. A large amount of debris material still stays in the Yusui Stream, which implies that same disaster may reoccur in the near future. From an engineering perspective, it is noted that the bridge safety after reconstruction. Increasing the height of bridge pillars to 20–25 m is recommended. However, the stability of the bridge pillars might be another issue. An alternative solution is a movable bridge. The bridge deck could be lifted during the massive debris flow mobilization. Another long-term solution is to replace the bridge with a submerged tunnel passing beneath the river bed.

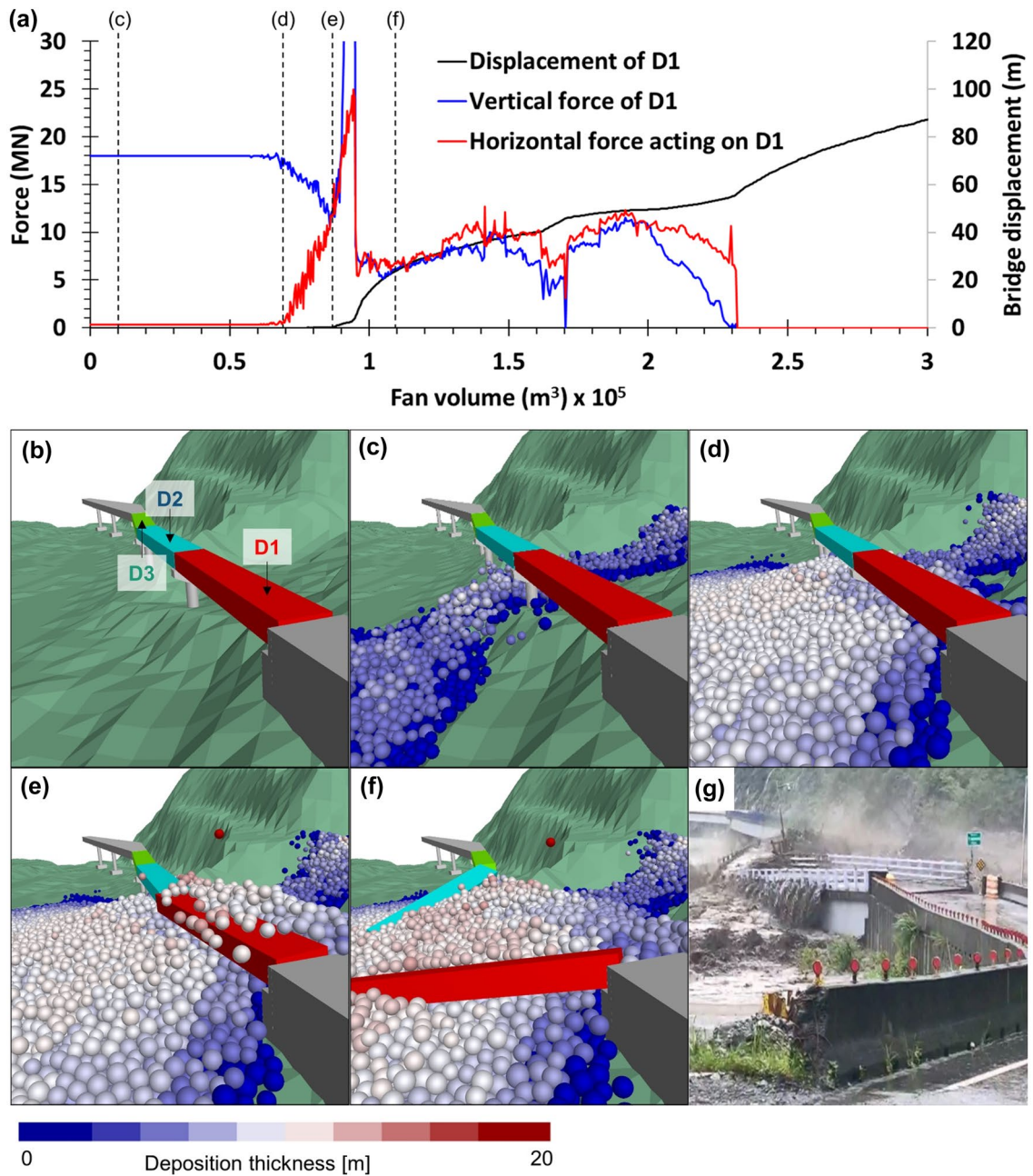


Fig. 18 **a** Evolution of force and displacement of bridge deck D1 and snapshots of fluid–structure interaction taken at different stages, including **b** initial stage, **c** fan initiation, **d** on-set of horizontal force

on deck D1, **e** deck D1 at critical stage to wash out, **f** wash out of decks D1 and D2, and **g** real image representing the deck wash out

Fig. 19 Evolution of alluvial fan formation

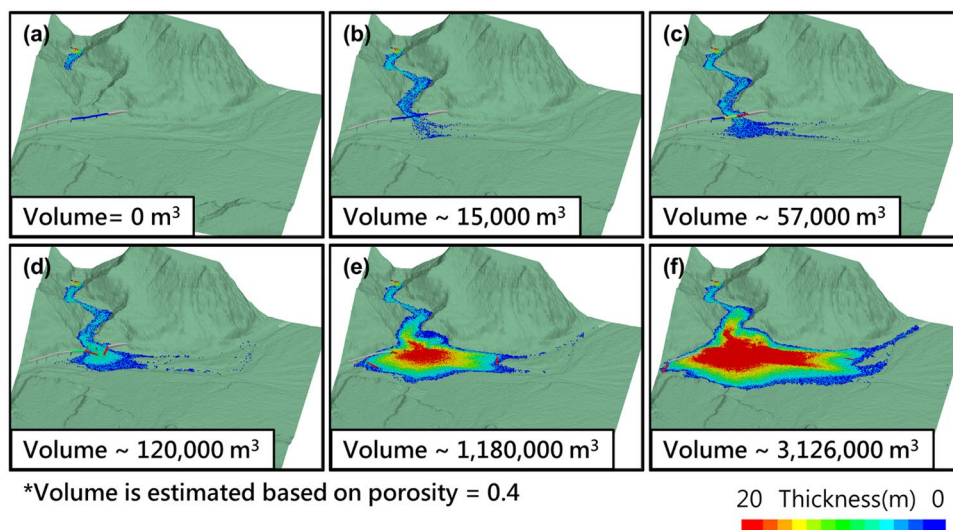
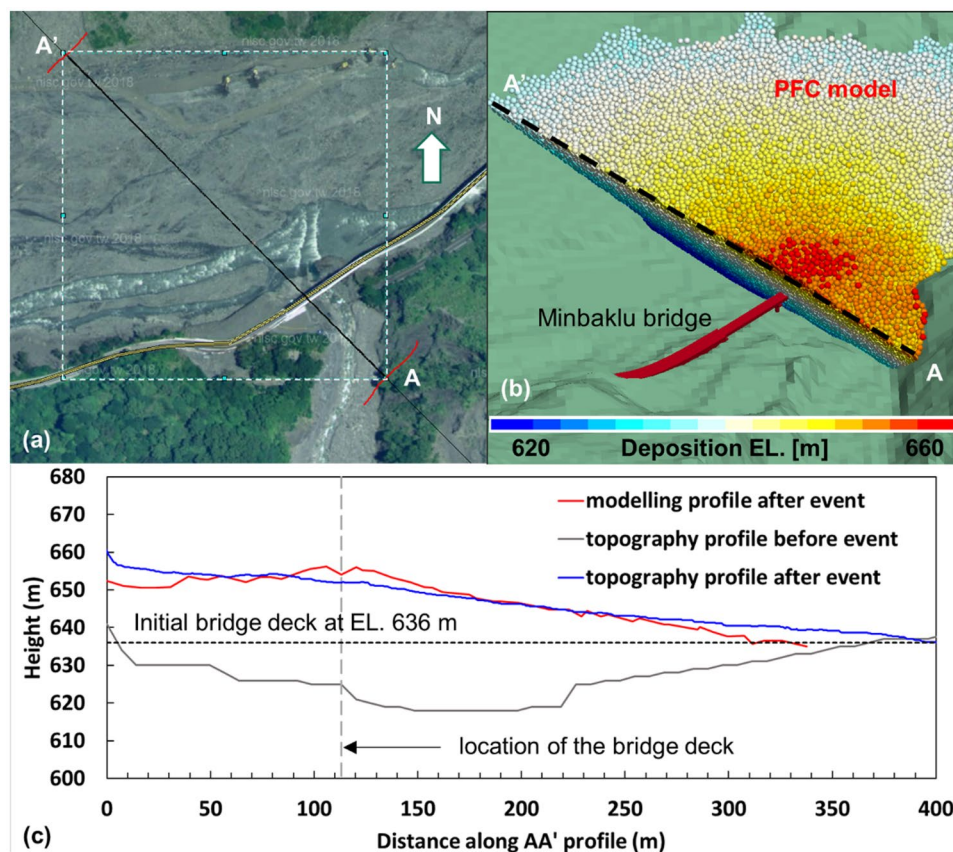


Fig. 20 Comparison of the deposition evolution through profile A-A' (a) location of the predefined profile (b) deposition in the PFC model (c) comparison between topography profile and modelling profile



Conclusion

To elucidate the development of debris flow in the Yusui Stream and the collapse event to the Minbaklu Bridge in 2021, this study proposed a hybrid model combining PFC and RAMMS to simulate the event through three stages: formation of the natural dam, debris flow triggered by dam braking, and bridge collapse owing to debris flow. To provide a credible database for the following simulation, first, the following analyses were conducted: (1) analyzing the

precipitation data, (2) identifying the geological background, (3) comparing the historical evolution of the landslide, (4) building digital terrain and performing the spatial analysis, and (5) investigating the seismic waveform to acquire the exact disaster timeline.

The simulation results indicate the following: (1) the time series of the natural dam simulation is consistent with the seismic waveform inversion; (2) the height of the natural dam in the simulation is approximately 74 m in height, which fits the result of the

spatial analysis; (3) the results of the RAMMS simulation and the spatial analysis both reveal that the erosion developed at the river bed of the flow region; (4) the RAMMS-PFC coupling can simulate the process of the failure of the Minbaklu Bridge, which revealed that the bridge was uplifted before being pushed away; (5) the final shape of the alluvial fan deposition is close in the post-disaster digital surface model, PFC, and RAMMS analysis. Overall, the proposed hybrid model is expected to function as a useful tool for investigating debris flow and interaction with engineering structures.

The simulation of this study was conducted to clarify the failure process of the disaster event and also provide essential information to the authority or engineering department for further planning of disaster mitigation and reconstruction of engineering structures. Moreover, a good simulation result depends on reliable data from field investigation, and thus, in the future, in-depth data such as in situ tests, borehole data, and laboratory experiments should be implemented to enhance the simulation results.

Acknowledgements

The authors acknowledge the Institute of Earth Science (IES) of Academia Sinica (AS), Taiwan, for the broadband seismic waveforms. The authors also acknowledge Prof. Ming-Lang Lin for his precious suggestion to this study.

Funding

This research received financial support from the Ministry of Science and Technology, Taiwan, under Contracts MOST 109-2124-M-027-001, MOST 110-2124-M-027-001, and MOST 111-2124-M-027-001. The deployment of temporal seismic networks was funded by MOST (MOST 110-2636-M-009-001) and AS (AS-TP-109-M08).

Declarations

Conflict of interest The authors declare no competing interests.

References

- Abraham MT, Satyam N, Pradhan B, Tian H (2022) Debris flow simulation 2D (DFS 2D): Numerical modelling of debris flows and calibration of friction parameters. *Journal of Rock Mechanics and Geotechnical Engineering*. <https://doi.org/10.1016/j.jrmge.2022.01.004>
- Berger C, McArdell BW, Schlunegger F (2011) Direct measurement of channel erosion by debris flows, Illgraben, Switzerland. *Journal of Geophysical Research: Earth Surface* 116. <https://doi.org/10.1029/2010JF001722>
- Borykov T, Mège D, Mangeney A et al (2019) Empirical investigation of friction weakening of terrestrial and Martian landslides using discrete element models. *Landslides* 16:1121–1140. <https://doi.org/10.1007/s10346-019-01140-8>
- Chang CW, Lin PS, Tsai CL (2011) Estimation of sediment volume of debris flow caused by extreme rainfall in Taiwan. *Eng Geol* 123:83–90. <https://doi.org/10.1016/j.enggeo.2011.07.004>
- Chen CH, Chao WA, Wu YM et al (2013) A seismological study of earthquakes using a real-time broad-band seismic network. *Geophys J Int* 194:885–898. <https://doi.org/10.1093/gji/ggt121>
- Chen CY (2016) Landslide and debris flow initiated characteristics after typhoon Morakot in Taiwan. *Landslides* 13:153–164. <https://doi.org/10.1007/s10346-015-0654-6>
- Chen H, Dadson S, Chi YG (2006) Recent rainfall-induced landslides and debris flow in northern Taiwan. *Geomorphology* 77:112–125. <https://doi.org/10.1016/j.geomorph.2006.01.002>

- Chen H, Petley D (2005) The impact of landslide and debris flows triggered by Typhoon Mindulle in Taiwan. *Quarterly Journal of Engineering Geology and Hydrogeology - Q J ENG GEOL HYDROGEOL* 38:301–304. <https://doi.org/10.1144/1470-9236/04-077>
- Chiu CC, Weng MC (2019) DEM simulation of planar sliding using a particulate interface model considering velocity-dependent friction. *Comput Geotech* 112:51–59. <https://doi.org/10.1016/j.compgeo.2019.04.001>
- Chiu CC, Weng MC, Huang TH (2015) Biconcave bond model for cemented granular material. *Journal of GeoEngineering* 10:91–103. [https://doi.org/10.6310/jog.2015.10\(3\).3](https://doi.org/10.6310/jog.2015.10(3).3)
- Chou HT, Lee CF (2009) Cross-sectional and axial flow characteristics of dry granular material in rotating drums. *Granular Matter* 11:13–32. <https://doi.org/10.1007/s10035-008-0118-y>
- Chou HT, Lee CF (2011) Falling process of a rectangular granular step. *Granular Matter* 13:39–51. <https://doi.org/10.1007/s10035-010-0221-8>
- Chou HT, Lee CF, Huang CH, Chang YL (2013) The monitoring and flow dynamics of gravelly debris flows. *Journal of Chinese Soil and Water Conservation* 44:144–157
- Chou HT, Lee CF, Lo CM (2017) The formation and evolution of a coastal alluvial fan in eastern Taiwan caused by rainfall-induced landslides. *Landslides* 14:109–122. <https://doi.org/10.1007/s10346-016-0678-6>
- Christen M, Kowalski J, Bartelt P (2010) RAMMS: numerical simulation of dense snow avalanches in three-dimensional terrain. *Cold Reg Sci Technol* 63:1–14. <https://doi.org/10.1016/j.coldregions.2010.04.005>
- Cuomo S, Moretti S, Aversa S (2019) Effects of artificial barriers on the propagation of debris avalanches. *Landslides* 16:1077–1087. <https://doi.org/10.1007/s10346-019-01155-1>
- Cuomo S, Perna AD, Martinelli M (2021) Material point method (MPM) hydro-mechanical modelling of flows impacting rigid walls. *Can Geotech J* 58:1730–1743. <https://doi.org/10.1139/cgj-2020-0344>
- Dai Z, Huang Y, Cheng H, Xu Q (2017) SPH model for fluid–structure interaction and its application to debris flow impact estimation. *Landslides* 14:917–928. <https://doi.org/10.1007/s10346-016-0777-4>
- Dai Z, Wang F, Yang H, Qin S (2020) Numerical investigation on the kinetic characteristics of the Yigong landslide in Tibet, China. *Nat Hazards Earth Syst Sci Discuss* 2020:1–25. <https://doi.org/10.5194/nhess-2020-289>
- Di Felice R (1994) The voidage function for fluid-particle interaction systems. *Int J Multiph Flow* 20:153–159. [https://doi.org/10.1016/0301-9322\(94\)90011-6](https://doi.org/10.1016/0301-9322(94)90011-6)
- Frank F, McArdell B, Huggel C, Vieli A (2015) The importance of erosion for debris flow runout modelling from applications to the Swiss Alps. *Natural Hazards and Earth System Sciences Discussions* 3:2379–2417. <https://doi.org/10.5194/nhessd-3-2379-2015>
- Frank F, McArdell BW, Oggier N et al (2017) Debris-flow modeling at Meretschibach and Bondasca catchments, Switzerland: sensitivity testing of field-data-based entrainment model. *Nat Hazard* 17:801–815. <https://doi.org/10.5194/nhess-17-801-2017>
- Hsieh ML, Capart H (2013) Late Holocene episodic river aggradation along the Lao-nong River (southwestern Taiwan): an application to the Tseng-wen Reservoir Transbasin Diversion Project. *Eng Geol* 159:83–97. <https://doi.org/10.1016/j.enggeo.2013.03.019>
- Huang C, Byrne TB, Ouimet WB et al (2016) Tectonic foliations and the distribution of landslides in the southern Central Range. *Taiwan Tectonophysics* 692:203–212. <https://doi.org/10.1016/j.tecto.2016.06.004>
- Hussin HY, Quan Luna B, van Westen CJ et al (2012) Parameterization of a numerical 2-D debris flow model with entrainment: a case study of the Faucon catchment, Southern French Alps. *Nat Hazards Earth Syst Sci* 12:3075–3090. <https://doi.org/10.5194/nhess-12-3075-2012>
- Jan C-D, Chen CL (2005) Debris flows caused by Typhoon Herb in Taiwan. In: Jakob M, Hungr O (eds) *Debris-flow Hazards and Related Phenomena*. Springer, Berlin Heidelberg, Berlin, Heidelberg, pp 539–563
- Lee CF, Huang CM, Tsao TC et al (2016) Combining rainfall parameter and landslide susceptibility to forecast shallow landslide in Taiwan. *Geotechnical Engineering Journal of the SEAGS & AGSSEA* 47:72–82
- Li X, Zhao J, Kwan JSH (2020) Assessing debris flow impact on flexible ring net barrier: a coupled CFD-DEM study. *Comput Geotech* 128:103850. <https://doi.org/10.1016/j.compgeo.2020.103850>

- Lin CH, Lin ML (2015) Evolution of the large landslide induced by Typhoon Morakot: a case study in the Butangbunasi River, southern Taiwan using the discrete element method. *Eng Geol* 197:172–187. <https://doi.org/10.1016/j.enggeo.2015.08.022>
- Lin JY, Yang MD, Lin BR, Lin P-S (2011) Risk assessment of debris flows in Songhe Stream. *Taiwan Engineering Geology* 123:100–112. <https://doi.org/10.1016/j.enggeo.2011.07.003>
- Lin ML, Jeng FS (2000) Characteristics of hazards induced by extremely heavy rainfall in Central Taiwan — Typhoon Herb. *Eng Geol* 58:191–207. [https://doi.org/10.1016/S0013-7952\(00\)00058-2](https://doi.org/10.1016/S0013-7952(00)00058-2)
- Lo CM (2017) Evolution of deep-seated landslide at Putanpunas stream. *Taiwan Geomatics, Natural Hazards and Risk* 8:1204–1224. <https://doi.org/10.1080/19475705.2017.1309462>
- Lo CM, Lin ML, Tang CL, Hu JC (2011) A kinematic model of the Hsiaolin landslide calibrated to the morphology of the landslide deposit. *Eng Geol* 123:22–39. <https://doi.org/10.1016/j.enggeo.2011.07.002>
- Lo CM, Weng MC, Lin ML et al (2018) Landscape evolution characteristics of large-scale erosion and landslides at the Putanpunas Stream. *Taiwan Geomatics, Natural Hazards and Risk* 9:175–195. <https://doi.org/10.1080/19475705.2017.1414079>
- Salm B (1993) Flow, flow transition and runout distances of flowing avalanches. *Annals of Glaciology* 18:221–226. <https://doi.org/10.3189/S0260305500011551>
- Schraml K, Thomschitz B, McArdell BW et al (2015) Modeling debris-flow runout patterns on two alpine fans with different dynamic simulation models. *Nat Hazard* 15:1483–1492. <https://doi.org/10.5194/nhess-15-1483-2015>
- Schürch P, Densmore AL, Rosser NJ et al (2011) Detection of surface change in complex topography using terrestrial laser scanning: application to the Illgraben debris-flow channel. *Earth Surf Proc Land* 36:1847–1859. <https://doi.org/10.1002/esp.2206>
- Voellmy A (1964) On the Destructive Force of Avalanches. *Forest Service*
- Weng MC, Chang CY, Jeng FS, Li HH (2020) Evaluating the stability of anti-dip slate slope using an innovative failure criterion for foliation. *Eng Geol* 275:105737. <https://doi.org/10.1016/j.enggeo.2020.105737>
- Weng MC, Lin ML, Lo CM et al (2019) Evaluating failure mechanisms of dip slope using a multiscale investigation and discrete element modelling. *Eng Geol* 263:105303. <https://doi.org/10.1016/j.enggeo.2019.105303>
- Weng MC, Wu MH, Ning SK, Jou YW (2011) Evaluating triggering and causative factors of landslides in Lawnon River Basin. *Taiwan Engineering Geology* 123:72–82. <https://doi.org/10.1016/j.enggeo.2011.07.001>
- Xu BH, Yu AB (1997) Numerical simulation of the gas-solid flow in a fluidized bed by combining discrete particle method with computational fluid dynamics. *Chem Eng Sci* 52:2785–2809. [https://doi.org/10.1016/S0009-2509\(97\)00081-X](https://doi.org/10.1016/S0009-2509(97)00081-X)
- Yang CM, Chao WA, Weng MC, et al (2022) Outburst debris flow of Yusui Stream caused by a large-scale Silabaku landslide, Southern Taiwan. *Landslides*. <https://doi.org/10.1007/s10346-022-01888-6>
-
- Supplementary Information The online version contains supplementary material available at <https://doi.org/10.1007/s10346-022-01963-y>.
-
- Springer Nature or its licensor holds exclusive rights to this article under a publishing agreement with the author(s) or other rightsholder(s); author self-archiving of the accepted manuscript version of this article is solely governed by the terms of such publishing agreement and applicable law.
-
- Wen-Jie Shiu**
Geotechnical Engineering Research Center, Sinotech Engineering Consultants Inc, Taipei, Taiwan
- Ching-Fang Lee · Chun-Yuan Liu · Wei-Kai Huang**
Disaster Prevention Technology Research Center, Sinotech Engineering Consultants Inc, Taipei, Taiwan
- Chia-Chi Chiu** (✉)
Institute of Mineral Resources Engineering, National Taipei University of Technology, Taipei, Taiwan
Email: ccchiu@ntut.edu.tw
- Meng-Chia Weng · Wei-An Chao**
Department of Civil Engineering, National Yang Ming Chiao Tung University, Hsinchu, Taiwan
- Che-Ming Yang**
Department of Civil and Disaster Prevention Engineering, National United University, Miaoli, Taiwan
- Cheng-Han Lin**
Department of Civil Engineering, National Taiwan University, Taipei, Taiwan
- Wen-Jie Shiu · Ching-Fang Lee · Chia-Chi Chiu · Meng-Chia Weng · Che-Ming Yang · Wei-An Chao · Chun-Yuan Liu · Cheng-Han Lin · Wei-Kai Huang**
GeoPORT Working Group, Taipei, Taiwan
Email: ccchiu@ntut.edu.tw